Smectic Phase in a Colloidal Suspension of Semiflexible Virus Particles

Zvonimir Dogic and Seth Fraden

The Martin Fisher School of Physics, Brandeis University, Waltham, Massachusetts 02254
(Received 10 January 1996; revised manuscript received 26 June 1996)

Aqueous suspensions of micron-length, charged, semiflexible fd virus particles are studied experimentally in order to explore properties of the cholesteric-smectic phase transition in a system approximating flexible, hard rods. Through comparison of this system with (1) computer simulations of hard, rigid rods, (2) experiments on tobacco mosaic virus, a rigid, charged virus, and on pf1, a flexible, charged virus, and (3) with recent theories of the nematic-smectic transition in flexible rods, we argue that flexibility raises the volume fraction at the phase transition, lowers the ratio of the smectic periodicity to the contour length, and drives the transition first order. [S0031-9007(97)02745-2]

The study of hard rod systems, where the interparticle potential is dominated by steric repulsion, has recently been a subject of intensive theoretical investigation [1–3] and computer simulations [4], which proved that entropy alone is sufficient to form a smectic (Sm) liquid crystal. In a smectic, the particle density is periodic in one dimension parallel to the long axis of the molecules, while the interparticle correlations perpendicular to the axis are short ranged, so a smectic can be visualized as a periodic stack of two-dimensional liquids, shown in Fig. 1. In a hard rod nematic (N) of sufficient concentration, the
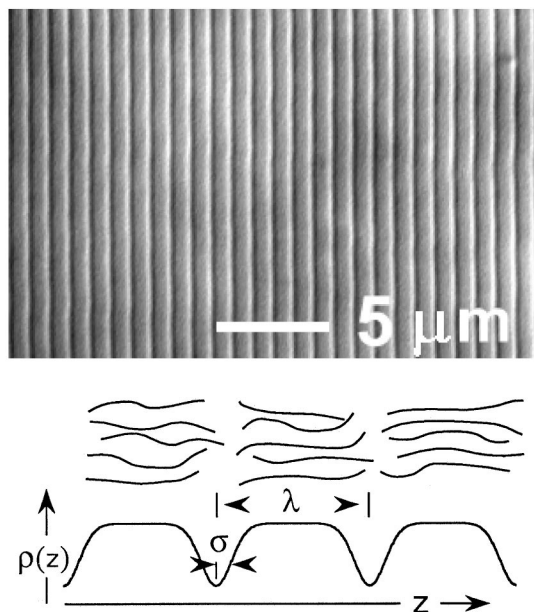

FIG. 1. Top: DIC optical micrograph of the fd smectic. The high contrast narrow black-white lines are the gaps between smectic layers. The half-width of the gap σ between layers is 90 nm and the smectic layer spacing λ is 920 nm. The particles lie in the plane of the photo and are oriented perpendicular to the smectic planes. Bottom: The upper part of the sketch shows the flexible fd molecules in the smectic phase. The lower portion is a plot of the fd density distribution $\rho(z)$ given in Eq. (1), as a function of distance z perpendicular to the smectic layers.

loss of entropy in forming smectic layers is more than compensated by the loss of excluded volume inside a layer [1,5,6]. For comparing this extensive body of theoretical work and simulations [1–9] to experiment, solutions of virus particles are the only physical system with interactions dominated by repulsion, which have a smectic phase [10–14].

We present and discuss experimental studies of the smectic phase of colloidal suspensions of rigid and flexible rodlike viruses. *Rigid* means that the persistence length P is much greater than the contour length L of the rod, while for the *flexible* rods we study $P \sim L$. All the virus particles studied are helical molecules with chiral symmetry, but for unknown reasons some viruses form nematics while others form cholesterics. When we refer to the rods as *achiral* this means that the suspension forms a nematic phase, while *chiral* molecules are those for which a cholesteric phase forms instead of a nematic.

We report measurements of the cholesteric-smectic (Ch-Sm) phase boundary in suspensions of fd, a charged, flexible, and chiral virus. When these experimental results are compared with the theory or simulation of hard, rigid, and achiral particles, we find that the fd Ch-Sm coexistence concentrations are higher, the transition in fd is discontinuous (first order) rather than continuous (second order), and the fd smectic layer spacing is smaller. These results and those of two other viruses are summarized in Table I below. The question is which of the three qualitative distinctions between the particles studied in simulations and theory (hard, rigid, and achiral) and fd (charged, flexible, and chiral) are responsible for the observed differences?

The bacteriophage fd is a particle of 880 nm in length (L), 6.6 nm in diameter (D), a persistence length (P) of 2200 nm, a charge density of about 10 e/nm in water at pH 7, and molecular weight of 1.64×10^7 g/M. The fd virus used in this study was grown and purified following standard recipes. To vary ionic strength, the virus was dialyzed against different molarities of TRIS-HCl buffer at pH 8.0 with 3 mM sodium azide added as a bacteriacide. All measurements were done at room temperature,

TABLE I. Molecular properties and phase behavior of three viruses and one computer model. The trends are that with increasing flexibility (a) the order of the N-Sm transition changes from 2nd to 1st, (b) the smectic layer spacing decreases, and (c) the volume fraction of the N-Sm boundary increases.

Particle	Charge	Chirality	Flexibility	Transition order	Smectic layer	Volume fraction
Simulation	None	Nematic	Rigid	2nd	$1.25-1.3L$	$\phi \sim 0.5$
TMV	$20\,e/\text{nm}$	Nematic	Rigid ($P > 10L$)	2nd	$1.1-1.2L$	
pf1	$10\,e/\text{nm}$	Nematic	Flexible ($P \sim L$)	1st	$1.05L$	
fd	$10\,e/\text{nm}$	Cholesteric	Flexible ($P \sim 2.5L$)	1st	$1.03L$	$\phi_{\text{eff}} = 0.75$

20 °C. Sample polydispersity was checked using gel electrophoresis on the intact virus, which showed a single sharp band indicating that the preparations were highly monodisperse. (See Refs. [14,15] for full details.)

Although the particles are charged, it is possible to account for the electrostatic repulsion by considering the particles to have a larger, effective hard rod diameter determined by calculating the excluded volume of a pair of rods averaged over their angular distribution function [3, 14–17]. Since crossed charged rods have a lower energy than parallel rods, the effective diameter will depend on the angular distribution of rods and will be denoted as $D_{\text{eff}}^{\text{iso}}$ or $D_{\text{eff}}^{\text{nem}}$ when the rods are in the isotropic or nematic phases, respectively. In the isotropic phase the angular correlation between rods is short ranged [15], while in the nematic the rods are parallel, on average, to a given direction. Because of this the effective diameter will be larger in the nematic phase than in the isotropic phase. Salt added to the suspension screens the electric repulsion and decreases the effective diameter towards its hard rod value. Thus the charged fd system approximates a hard rod system where the diameter can be systematically varied by adjusting the suspension's ionic strength.

In Fig. 2 the phase diagram of fd as a function of ionic strength of the TRIS buffer at constant pH 8.0 is shown. The phase diagram was established by optical microscopy and light scattering measurements. The isotropic phase is optically isotropic, the cholesteric birefringent, and the smectic iridescent. Concentrations were determined using absorbence spectroscopy [14,15]. At low virus concentrations, the suspensions are isotropic (I) and with increasing fd mass concentration (ρ) a first-order phase transition to a cholesteric (Ch) phase is observed. The onset of the cholesteric phase occurs from 10–20 mg/ml of fd and the relative width of the I-Ch biphasic region $w = (\rho_{\text{Ch}} - \rho_{\text{I}})/\rho_{\text{I}}$ varies from 0.05–0.15 as the ionic strength is increased from 1 to 100 mM [15]. These experimental isotropic coexistence concentrations c_{I} accurately follow the Khokhlov-Semenov [18] (KS) prediction for hard, semiflexible, nematic polymers calculated by Chen [19] with $c_{\text{I}} = 4.7/b_{\text{eff}}$ and $b_{\text{eff}} = \pi L^2 D_{\text{eff}}^{\text{iso}}/4$. Because the free energy difference between the nematic (N) and cholesteric phases is small, the KS theory applies equally well to the I-Ch and I-N transitions. Both the width of the coexistence region and the coexistence concentrations differ significantly from the rigid rod pre-

dictions of $c_{\text{I}} = 3.3/b_{\text{eff}}$ and $w = 0.27$ [3]. Although fd is fairly rigid with $P/L = 2.5$, the flexibility is important enough to narrow the width of the coexistence region, w, by a factor of 3 from the rigid rod limit and suppress the isotropic-cholesteric transition to higher concentrations.

As the fd concentration is further increased a single phase cholesteric is formed, followed by an iridescent smectic phase. At still higher concentrations, the iridescence disappears, but the birefringence remains. X-ray scattering measurements of this "disordered" phase indicate that the interparticle correlations perpendicular to the particle axis (director) are short ranged and similar to the correlations in both the nematic phase created by unwinding the cholesteric with a magnetic field, as well as in the smectic phase. The disordered phase may be a nematic or a glass, and we have observed the disordered-smectic transition to be reversible when varying the fd concentration. Incidentally, this same effect has been observed with tobacco mosaic virus (TMV) [20]. This transition occurs at an effective volume fraction (defined below) $\phi_{\text{eff}} \sim 1$, larger than the real volume fraction $\phi \sim 0.1$, because of electrostatic repulsion. The large value of ϕ_{eff} suggests that charge destabilizes the smectic at high concentrations.
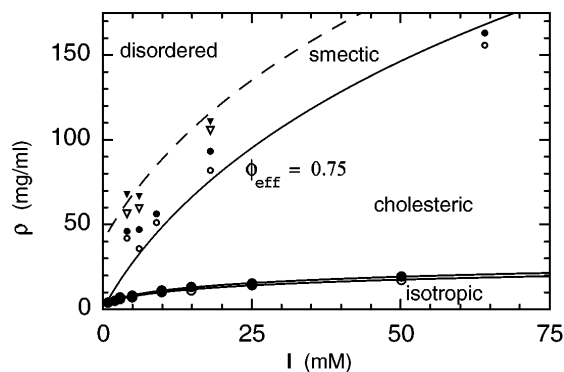

FIG. 2. fd shows a sequence of isotropic (I), cholesteric (Ch), smectic (Sm), and disordered with increasing concentration. Both the I-Ch and Ch-Sm transitions are first order. The nature of the disordered region is not understood. The solid line along the Ch-Sm boundary corresponds to a constant effective volume fraction of $\phi_{\text{eff}} = 0.75$. The open circles and triangles correspond to the highest measured concentrations of the cholesteric and smectic phases, respectively, while the solid triangles and circles correspond to the lowest measured concentrations of the disordered and smectic phases, respectively. The dashed line is a guide to the eye separating the disordered-smectic phases.

Along the cholesteric-smectic coexistence line we find $\phi_{\text{eff}} = c_s V_{\text{eff}} = 0.75 \pm 0.05$ with $V_{\text{eff}} = \pi L (D_{\text{eff}}^{\text{nem}})^2 / 4$ with c_s the number density of fd at the cholesteric-smectic phase boundary, and with V_{eff} and $D_{\text{eff}}^{\text{nem}}$ the effective volume and diameter of the rods in the nematic phase. The spread in values of V_{eff} comes from choosing two different values for the order parameter of the nematic, $S = 0.8$ and $S = 0.9$. These values are consistent with our x-ray measurements of the order parameter in magnetically aligned samples of concentration near the Ch-Sm transition. $D_{\text{eff}}^{\text{nem}}$ is calculated using the second virial coefficient in the Onsager theory: $D_{\text{eff}}^{\text{nem}} = D_{\text{eff}}^{\text{iso}}[1 + h\eta(f)/\rho(f)]$ with h the twist parameter, and both η and ρ functions of the angular distribution in the nematic phase [21]. The above definition of an effective diameter will be valid as long as the average angle $\sqrt{\langle \theta^2 \rangle}$ between particles in the nematic phase is greater than $D_{\text{eff}}^{\text{nem}}/L$ (see Sec. 2.3 of Ref. [3]). We find for an angular distribution function with an order parameter of $S = 0.9$ [3] that $\sqrt{\langle \theta^2 \rangle} \sim 10 D_{\text{eff}}^{\text{nem}}/L$ for the largest value of $D_{\text{eff}}^{\text{nem}}$. Although the effective diameter diverges for long, strictly parallel charged rods, for fd with $S = 0.9$ with a twist constant $h = 0.15$, we find $D_{\text{eff}}^{\text{nem}} = 1.12 D_{\text{eff}}^{\text{iso}}$. But since S increases with concentration, the concept of $D_{\text{eff}}^{\text{nem}}$ becomes invalid at concentrations above the Ch-Sm coexistence.

Figure 1 shows an optical microscopy photograph obtained using differential interference contrast (DIC) [22] of the individual molecular layers of the smectic phase. The photographs were taken on a Nikon Microphot SA using a 60X objective lens and a condenser, each with a 1.4 numerical aperture. The illumination source was a 100 W mercury lamp with an Ellis fiber scrambler. The sample was 5 μm thick and was contained between a microscope slide and a cover slip. The images were collected with a CCD video camera and the only video processing was the analog offset and gain of the DAGE-MTI CCD72 video camera. The fd particles lie in the plane of the photo and are oriented perpendicular to the layer lines. The asymmetric intensity variation in the photograph suggests a model of the virus density $\rho(z)$ in the smectic phase as being of uniform density separated by a narrow gap between layers of lower virus density. We model the density of ends of the virus particles in the gaps as having a Gaussian distribution, illustrated in Fig. 1,

$$\rho(z) = \rho_0 - \rho_1 \sum_n \delta(z - n\lambda) \otimes e^{-z^2/2\sigma^2}, \quad (1)$$

with n the integers, ρ_0 and ρ_1 constants, and σ the gap width. Because the smectic is periodic in only one dimension, thermal fluctuations destroy long range order and the intensity of scattered light from the smectic layers will not have true Bragg peaks, but instead algebraic singularities. The intensity of the scattered light from $\rho(z)$ is

$$I(q_z) \propto e^{-q_z^2 \sigma^2}(q_z - q_0 m)^{\eta-2}, \quad (2)$$

with q_z the scattered wave vector, $q_0 = 2\pi/\lambda$ with λ the smectic periodicity, m the diffraction order, and η [23] a function of the elastic moduli of the smectic phase

and also increasing proportional to m^2. The samples were in 0.7 mm diameter x-ray capillaries and typically had about 15° of mosaic spread. We observed five Bragg diffraction peaks in light scattering measurements from aligned smectic samples with 488 nm light, but the peak widths did not increase with increasing m, indicating that η is much smaller than 2. However, the intensity integrated over the mosaic spread of each peak did decrease according to Eq. (2), and we determined that the interlayer gap has a width of $\sigma = 90 \pm 10$ nm and $\lambda = 920 \pm 10$ nm. These values did not vary with ionic strength. The structure deduced from the model of Eqs. (1) and (2) is sketched in Fig. 1.

We measured the cholesteric pitch as a function of concentration over the entire cholesteric phase for several ionic strengths. With increasing concentration the pitch initially decreases as $c^{-\alpha}$, with α a function of ionic strength, decreasing systematically from $\alpha = 5/3$ at 64 mM to $\alpha = 1.1$ at 4 mM ionic strength. At higher concentrations, within 10% of the smectic phase, the cholesteric helix begins to unwind and the pitch increases slightly until the cholesteric-smectic phase transition occurs and the helix abruptly unwinds [14]. Helix unwinding in general is thought to be due to pretransitional smectic density fluctuations, but surprisingly there was no indication of such fluctuations for fd with either light scattering or optical microscopy measurements.

We now compare the above experimental results of the smectic phase of the semiflexible molecule fd with the results from simulations, theory, and experiments from suspensions of other rodlike viruses. We argued in the discussion of Fig. 2 that the volume fraction at the cholesteric-smectic transition was a constant $\phi_{\text{eff}} = 0.75 \pm 0.05$, even though L/D_{eff} increases from about 30 to 70 as the ionic strength varies from 4–65 mM. Theories and simulations show that the volume fraction at the smectic transition initially decreases with increasing L/D, but becomes constant above $L/D > 10$ [4,24], thus the independence of ϕ_{eff} on L/D_{eff} is expected. However, the observed ϕ_{eff} is substantially higher than calculated in simulations or theory of the N-Sm transition for rigid and hard particles, for which $\phi = \sim 0.5$ is found [3,9].

The Ch-Sm phase transition is first order, and when compared to an otherwise equivalent N-Sm transition, the cholesteric will transform to the smectic at a higher concentration than the nematic [25]. In a thermotropic liquid crystal, the smectic phase transition was shifted by less than 1% [26], not nearly enough to account for the high $\phi_{\text{eff}} = 0.75$ found for fd. Since both chirality and charge do not account for the high effective volume fraction, we are led to conclude that introducing flexibility acts to suppress the smectic phase transition. Recent theoretical work on hard, flexible, nematic rods bears out this conclusion [7–9]. These models are applicable to our experiments because chirality is negligible and the charged rods can be represented as hard rods with a larger effective diameter.

The light scattering and optical microscopy studies revealed that the ratio of smectic periodicity to fd contour length was $\lambda/L = 1.03$. Theory and simulations of hard cylinders have a much larger value $\lambda/L = 1.4$ [3], while experiments on TMV, a rigid, but charged cylinder has $\lambda/L = 1.1-1.2$ [12,13]. The shape of the particles has a strong effect on the layer spacing and volume fraction of the smectic phase. Rounding the ends of hard, rigid cylinders both raises ϕ and lowers λ/L [24], and in the case of an ellipsoid of revolution the smectic phase is completely suppressed [6]. Since λ/L is even smaller for fd than for TMV, we conclude that flexibility lowers λ/L compared to rigid particles.

The combination of a lack of pretransitional density fluctuations, the large discontinuous increase in the scattered light intensity, and sudden unwinding of the cholesteric helix at the cholesteric-smectic phase boundary indicates that the Ch-Sm transition is first order, as expected theoretically [25].

We have also studied another viral system, pf1. This virus is 2 μm in length and is structurally similar to fd, but has a nematic-smectic transition [11] instead of a cholesteric-smectic transition. Using optical microscopy we observed coexisting regions of the nematic and smectic phases with abrupt boundaries between the phases, which is evidence of a first-order transition. We also note the absence of detectable pretransitional smectic density fluctuations, in contrast to the simulations of hard, rigid particles [4] and the experiments on the rigid TMV where in both cases the nematic to smectic transition is second order [13,20]. All three viruses are charged and it seems the only significant difference between them is flexibility (Table I). We conclude that flexibility drives the second order N-Sm transition first order, in agreement with a recent calculation [8].

Our work focuses on the effect of persistent flexibility on the smectic phase transition in a lyotropic liquid crystal. We find that when compared with rigid particles, flexibility raises the volume fraction at the phase transition, lowers the ratio of the smectic periodicity to the contour length, and drives the transition first order. This work raises several fundamental questions recently addressed [7–9]: How much flexibility is needed to change the nematic-smectic transition from second to first order? How flexible can a persistent polymer be and still produce a smectic phase?

The destabilization of the smectic at high concentrations, where the second virial calculation is invalid, for both rigid and flexible viruses remains unexplained, and we suggest that the effect of charge on the nematic-smectic transition should be explored theoretically.

[1] M. Hosino, H. Nakano, and H. Kimura, J. Phys. Soc. Jpn. **59**, 740 (1979).

[2] D. Frenkel, in *Liquids, Freezing, and Glass Transition,* edited by J. P. Hansen, D. Levesque, and J. Zinn-Justin (North-Holland, Amsterdam, 1991), pp. 689–762.

[3] G. J. Vroege and H. N. W. Lekkerkerker, Rep. Prog. Phys. **8**, 1241 (1992).

[4] A. Stroobants, H. N. W. Lekkerkerker, and D. Frenkel, Phys. Rev. A **36**, 2929 (1987).

[5] X. Wen and R. B. Meyer, Phys. Rev. Lett. **59**, 1325 (1987).

[6] B. Mulder, Phys. Rev. A **35**, 3095 (1987).

[7] P. van der Schoot, J. Phys. II (France) **6**, 1557 (1996).

[8] A. V. Tkachenko, Phys. Rev. Lett. **77**, 4218 (1996).

[9] P. Bladon and D. Frenkel, J. Phys. Condens. Matter **47**, 9445 (1996).

[10] J. Lapointe and D. A. Marvin, Mol. Cryst. Liquid Cryst. **19**, 269 (1973).

[11] F. P. Booy and A. G. Fowler, Int. J. Biol. Macromol. **7**, 327 (1985).

[12] X. Wen, R. B. Meyer, and D. L. D. Caspar, Phys. Rev. Lett. **63**, 2760 (1989).

[13] J. H. Wang, F. Lonberg, X. Ao, and R. B. Meyer, in *Ordering in Macromolecular Systems,* edited by A. Teramoto, M. Kobayashi, and T. Norisuje (Springer-Verlag, Berlin, 1994).

[14] S. Fraden, in *Observation, Prediction, and Simulation of Phase Transitions in Complex Fluids,* edited by M. Baus, L. F. Rull, and J. P. Ryckaert (Kluwer Academic Publishers, Dordrecht, 1995), p. 113.

[15] J. Tang and S. Fraden, Liq. Cryst. **19**, 459 (1995).

[16] L. Onsager, Ann. N.Y. Acad. Sci. **51**, 627 (1949).

[17] A. Stroobants, H. N. W. Lekkerkerker, and T. Odijk, Macromolecules **19**, 2232 (1986).

[18] A. R. Khokhlov and A. N. Semenov, Physica (Amsterdam) **112A**, 605 (1982).

[19] Z. Y. Chen, Macromolecules **26**, 3419 (1993).

[20] Jinhua Wang, Ph.D. thesis, Brandeis University, 1996.

[21] The definitions of h, ρ, and η are in Sec. 2.6 of Ref. [3]. The functions ρ and η are tabulated in Ref. [17], and the values for h and $D_{\text{eff}}^{\text{iso}}$ for fd are taken from Ref. [15]. The twist constant h is always less than 0.15 for our fd samples.

[22] S. Inoue, Methods Cell Biol. **30**, 85 (1989).

[23] C. R. Safinya *et al.,* Phys. Rev. Lett. **57**, 2718 (1986).

[24] G. T. Evans, Mol. Phys. **76**, 1359 (1992).

[25] T. C. Lubensky, J. Phys. (Paris), Colloq. **1-36**, C151 (1975).

[26] D. Dolphin, Z. Muljiani, J. Cheng, and R. B. Meyer, J. Chem. Phys. **58**, 413 (1973).